

Improved photovoltaic performance of InGaN single junction solar cells by using *n-on-p* type device structure

M. SONG^a, Z. WU^{a,b*}, Y. FANG^a, R. XIANG^a, Y. SUN^a, H. WANG^a, C. YU^a, H. XIONG^a, J. DAI^{a,b}, C. CHEN^{a,b}

^aWuhan National Laboratory for Optoelectronics, School of Optoelectronic Science and Engineering, Huazhong University of Science and Technology, Wuhan 430074, China

^bState Key Laboratory of Functional Materials for Informatics, Shanghai Institute of Microsystem and Information Technology, Chinese Academy of Sciences, 865 Changning Road, Shanghai 200050, China

The performance of In_{0.65}Ga_{0.35}N single junction solar cell including an InGaN window layer with p-on-n and n-on-p two types of configurations has been theoretically investigated. By taking polarization effects into consideration, it is found that with the same dislocation density the n-on-p type cell has a very high conversion efficiency, while the energy conversion efficiency of the conventional p-on-n type cell is very low. The superior performance of the n-on-p type cell is due to a better carrier collection efficiency resulting from an improved band alignment at the interface between the In_{0.65}Ga_{0.35}N emitter layer and the InGaN window layer, as compared to the n-on-p structure. The effects of dislocation density on the n-on-p type In_{0.65}Ga_{0.35}N solar cell efficiency have been evaluated and are compared with the case of the GaAs solar cell, showing that the InGaN solar cell has a greater tolerance level to the dislocation density than GaAs solar cell, which is very similar to the case for the light-emitting diodes.

(Received June 17, 2010; accepted July 14, 2010)

Keywords: InGaN; *n-on-p* structure; polarization effect; solar cell

1. Introduction

The band gap of InGaN alloys can be continually tuned in the range of 0.7 to 3.4 eV, spanning nearly the entire solar spectrum, therefore the InGaN system is considered as a promising candidate for fabricating high efficiency single and multi-junction solar cells [1]. Its superior resistance against high-energy particle radiation also makes InGaN based solar cells especially suitable for space applications [2]. Since InGaN was first proposed to use for solar cell applications, enormous efforts have been made in material epitaxial growth and device design of InGaN solar cells [3-6]. However, the performance of InGaN based solar cells is still very poor; one recent work reported a 0.05% conversion efficiency under AM1.5 illumination for InGaN (~2.67 eV) single junction solar cell with GaN window layer [7]. Two important issues have to be considered before we can fully implement the InGaN alloys for photovoltaic applications. First, due to their hexagonal wurtzite structure, InGaN alloys have strong spontaneous and piezoelectric polarizations that are inherent to these wurtzite semiconductors due to their non-centrosymmetry and the strain [8]. Polarization discontinuities in III-nitride devices can result in potential barrier and band bending, causing the deleterious quantum confined Stark effect in the InGaN quantum well for LEDs applications, and inducing a beneficial high density of

two-dimensional electron gas at the AlGaIn/GaN interface for applications in high electron mobility transistors. Similarly, presence of the high polarization fields could be beneficial or adverse to the collection of free carriers, and thus devices should be properly designed to alleviate or utilize constructively the polarization effect. Another important issue is that high density of threading dislocations exists in III-nitrides epilayers at levels of $\sim 1 \times 10^9$ /cm², which is mainly caused by the large lattice mismatch with the sapphire substrates, and are more than four orders of magnitude higher than in typical III-V compound semiconductors. Such high density of threading dislocations could lead to poor device performance in photovoltaic devices based on previous experiences from conventional silicon or III-V semiconductors. However, defects in the InGaN system do not seem to adversely affect the performance or the lifetimes of LED devices. Indeed, blue LEDs manufactured from InGaIn alloys have very high efficiency and very long lifetimes [9]. If InGaN solar cells behave like LEDs, high defect densities may have a negligible effect on device efficiency. Therefore it is very important to know the defect tolerance level of InGaN based solar cells.

In this work, first we have shown that *n-on-p* type cell structure instead of *p-on-n* type one should be used to achieve highly efficient InGaN single solar cells if the polarization effects are taken into account. Then we have

investigated the performance of the *n-on-p* type InGaN single junction solar cell as the function of dislocation densities, and have found that the defect tolerance level of InGaN solar cell is greater than that of GaAs solar cell, with high promise to make high efficiency solar cells from InGaN material system.

2. Physical models and device simulations

A two dimensional finite element analysis and modeling software for semiconductor optoelectronic devices, Crosslight APSYS simulator, is used in our simulation [10]. It can offer the calculation of the optical and electrical properties by solving mainly the Poisson's equation and carrier drift-diffusion equation with some necessary material parameters. Required physical properties for APSYS simulator are mobility, intrinsic carrier concentration, intrinsic absorption coefficient, band-to-band radiative recombination lifetime, Auger recombination lifetime, and so on. Physical properties of InGaN cells are included in the APSYS internal parameter base, except the mobility, carrier lifetime and absorption coefficient. Since there is no experimental data available for the minority carrier mobility of n- and p-In_{0.65}Ga_{0.35}N in the literature, the dependence of minority carrier mobility for n- and p- In_{0.65}Ga_{0.35}N on carrier concentrations at room temperature (300 K) was assumed to be described by the simple semi-empirical analytical model proposed for low-field mobility of GaN [11]:

$$\text{For electron mobility,} \quad \mu_e = 55 + \frac{945}{1 + (N_A/2 \times 10^{17})} \text{ cm}^2 \text{ eV}^{-1} \text{ s}^{-1}, \quad (1)$$

$$\text{For hole mobility,} \quad \mu_h = 3 + \frac{167}{1 + (N_D/3 \times 10^{17})} \text{ cm}^2 \text{ eV}^{-1} \text{ s}^{-1}, \quad (2)$$

where N_A , N_D are the doping level of p type and n type In_{0.65}Ga_{0.35}N, respectively. It should be noted that this model included the contributions from phonon scattering and impurity scattering, and the effect of dislocation scattering on carrier mobility was neglected.

The presence of threading dislocation affects carrier lifetime and thus diffusion lengths, therefore the effect of dislocation density on the InGaN cell performance can be evaluated by first considering the variation of carrier lifetime with the dislocation density. There are mainly three channels for carrier recombination: radiative recombination, Auger recombination and dislocation-induced recombination. And the minority carrier lifetime τ can be defined by

$$\begin{aligned} \frac{1}{\tau} &= \frac{1}{\tau_{\text{radiative}}} + \frac{1}{\tau_{\text{dislocation}}} + \frac{1}{\tau_{\text{Auger}}} \\ &= B_{\text{radiative}} N + B_{\text{Auger}} N^2 + \left(\pi^3 N_d \frac{D}{4} \right), \end{aligned} \quad (3)$$

where $B_{\text{radiative}}$ and B_{Auger} are radiative and Auger recombination coefficient, respectively, N_d dislocation density, N the carrier concentration of n- or p-type layer, and $D = \mu \frac{KT}{e}$ is defined as minority carrier diffusion coefficient for electron in p-type layer or hole in n-type layer.

For the InGaN single junction solar cell, when the energy E of photon is higher than the bandgap E_g of InGaN, the absorption coefficient of InGaN can be obtained by the following equation cited from reference 6:

$$\alpha(\mu\text{m}^{-1}) = 7.91(E - E_g)^4 - 14.9(E - E_g)^3 + 5.32(E - E_g)^2 + 9.61(E - E_g) + 1.98 \quad (4)$$

and the corresponding bandgap can be calculated by the bowing equation [12]:

$$E_g = 0.7 \cdot x + 3.4 \cdot (1 - x) - b \cdot x \cdot (1 - x), \quad (5)$$

where b , 1.43 eV, is obtained as the best-fit bowing parameter. In_{0.65}Ga_{0.35}N alloy with a bandgap of 1.32 eV, is selected as the active layer in our simulation since it has the best performance in the InGaN single junction cells.

Table 1. Lattice constants, spontaneous polarization, piezoelectric constants and elastic constants of InN and GaN used in the calculations of polarization effects of InGaN single junction solar cell from reference 8.

Parameter	GaN	InN
a (nm)	0.3189	0.354
P_{SP} (C /m ²)	-0.042	-0.034
e_{31} (C /m ²)	-0.57	-0.49
e_{33} (C /m ²)	0.97	0.73
C_{13} (GPa)	92	103
C_{33} (GPa)	224	405

The total macroscopic polarization P of InGaN is defined as the sum of the spontaneous polarization P_{SP} in the equilibrium lattice, and the strain-induced piezoelectric polarization P_{PE} . To calculate the amount of the polarization in dependence of the In-content x of the

$In_xGa_{1-x}N$, we use the following set of numeric interpolations between the physical properties of GaN and InN [8, 13]:

$$P_{SP} = P_{SP}^{InN} x + P_{SP}^{GaN} (1-x) - bx(1-x) \quad (6)$$

$$P_{PE} = 2 \frac{a(x) - a_0}{a_0} (e_{31} - e_{33} \frac{C_{13}}{C_{33}}), \quad (7)$$

where b is the bowing parameter, defined as -0.038 C/m^2 ; $a(x)$ and a_0 are the lattice constants of relaxed and pseudomorphically strained $In_xGa_{1-x}N$, respectively; e_{31} and e_{33} are piezoelectric constants; and C_{13} and C_{33} are elastic constants of the $In_xGa_{1-x}N$, which can also be obtained by the linear interpolation between the physical properties of GaN and InN (Table 1). Thus, at an abrupt interface of an InGaN top/bottom layer the polarization sheet charge density σ can be obtained by the following equation:

$$\sigma = (P_{SP} + P_{PE})_{top} - (P_{SP} + P_{PE})_{bottom}. \quad (8)$$

3. Results and discussion

Owing to the strong effect of polarization on the performance of electronic and optoelectronic devices, it is vital to design an effective device structure to obtain a high efficiency solar cell. First, we investigate a conventional p-on-n single junction $In_{0.65}Ga_{0.35}N$ solar cell, consisting of a $0.2 \mu\text{m}$ thick n- $In_{0.65}Ga_{0.35}N$ base layer with carrier concentration of $5 \times 10^{17} / \text{cm}^3$, a $0.1 \mu\text{m}$ p- $In_{0.65}Ga_{0.35}N$ emitter layer with carrier concentration of $2 \times 10^{18} / \text{cm}^3$, and a 10nm p- $In_{0.4}Ga_{0.6}N$ window layer with carrier concentration of $2 \times 10^{18} / \text{cm}^3$. The device structure and the corresponding band diagram are shown in figures 1 (a) and (b), respectively. The utilization of $In_{0.4}Ga_{0.6}N$ window layer is aimed to reduce loss of photo-generated minority carriers at the surface of the material due to the presence of surface states which arise from “dangling bonds,” chemical residues, metal precipitates, native oxides, and the like. Since the $In_{0.4}Ga_{0.6}N$ window is very thin, we assume it is pseudomorphically grown on $In_{0.65}Ga_{0.35}N$, and under tensile stress, inducing a piezoelectric polarization with the same sign as its spontaneous polarization. Assuming a lower dislocation density of $10^5 / \text{cm}^2$ in the conventional p-on-n single junction $In_{0.65}Ga_{0.35}N$ solar cell, the performance of this cell is calculated using solar spectrum of AM1.5 global, $100 \text{ mW} / \text{cm}^2$ at 300K, and is found to be extremely poor, with an energy conversion efficiency of 0.76%, an open-circuit voltage (V_{oc}) of 0.74 eV, a short-circuit current (J_{sc}) of 0.16 mA/cm^2 and a fill factor of 8.9%. Such poor efficiency mainly results from the strong downward bending of bands at the hetero-interface of the strained

p- $In_{0.4}Ga_{0.6}N$ and the p- $In_{0.65}Ga_{0.35}N$ emitter layer as shown in the band diagram in figure 1 (b). According to the equation (6), (7) and (8), a high density of positive polarization sheet charge, $1.68 \times 10^{13} / \text{cm}^2$, is calculated at the hetero-interface, which induces the strong downward bending of bands with the two-dimensional electron gas at the interface. It acts as an energy barrier of more than 1.0 eV for photo-generated holes to overcome before reaching the electrodes. This problem is inevitable if InGaN window layer with lower In composition than that of $In_{0.65}Ga_{0.35}N$ has to be used for reducing the surface recombination velocity, and thus the p-on-n cell structure is not the right design for realizing high efficiency InGaN based solar cells. This conclusion could explain the very poor performance of InGaN solar as reported in reference 7, where the authors used the p-on-n type device structure with GaN window layer.

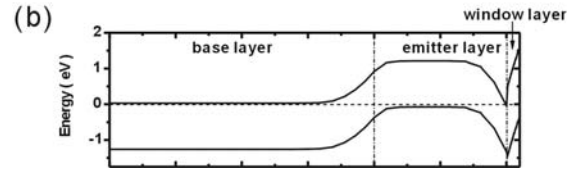
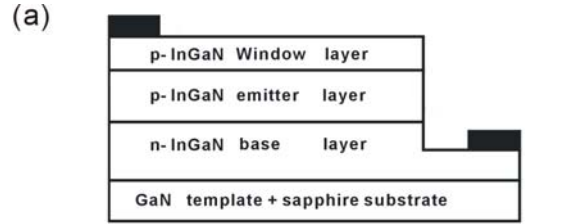


Fig. 1. Device structure (a) and band diagram (b) of the conventional p-on-n junction InGaN solar cell with p-InGaN window layer considering the polarization effects of InGaN films.

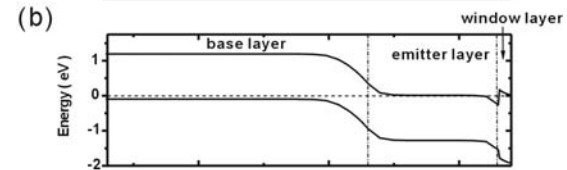
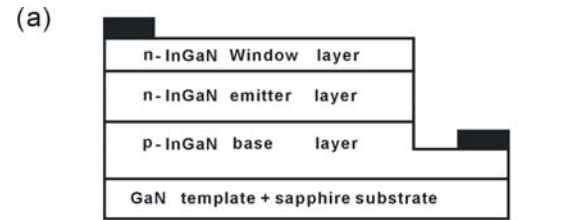


Fig. 2. Device structure (a) and band diagram (b) of the n-on-p junction InGaN solar cell with n-InGaN window layer considering the polarization effects of InGaN films.

Fig. 2 (a) and (b) show the device structure of n-on-p type InGaN single junction solar cell and the corresponding band diagram with the polarization effects, respectively. The n-on-p type InGaN single junction solar

cell consists of a $0.2 \mu\text{m}$ thick $p\text{-In}_{0.65}\text{Ga}_{0.35}\text{N}$ base layer with carrier concentration of $5 \times 10^{17} / \text{cm}^3$, a $0.1 \mu\text{m}$ $n\text{-In}_{0.65}\text{Ga}_{0.35}\text{N}$ emitter layer with carrier concentration of $2 \times 10^{18} / \text{cm}^3$, and a 10 nm $n\text{-In}_{0.4}\text{Ga}_{0.6}\text{N}$ window layer with carrier concentration of $2 \times 10^{18} / \text{cm}^3$. In this *n-on-p* type InGaN cell structure, the *n* type $\text{In}_{0.65}\text{Ga}_{0.35}\text{N}$ emitter is located above the *p* type base layer, and hence photo-generated electrons are the minority carriers that have to transport across the interface of the strained *n*-InGaN window layer and *n*-InGaN emitter layer before collection. Using the same lower dislocation density of $10^5 / \text{cm}^2$ as in the above conventional *p-on-n* single junction $\text{In}_{0.65}\text{Ga}_{0.35}\text{N}$ solar cell, the simulation results for the *n-on-p* InGaN cell structure shows that it has a high conversion efficiency of 20.8%, V_{oc} of 0.86 eV, J_{sc} of $28.61 \text{ mA} / \text{cm}^2$ and a fill factor of 85% under the same illumination, AM1.5 global, $100 \text{ mW} / \text{cm}^2$ at 300K. It indicates that a drastic performance boost has been achieved by adopting the *n-on-p* InGaN cell structure as compared to the conventional *p-on-n* scheme. The high efficiency of *n-on-p* InGaN cell structure can be understood from its band diagram as shown in figure 2 (b). In this device configuration, the polarization effect is beneficial to the collection of photo-generated electrons. With the positive polarization sheet charge density of $1.68 \times 10^{15} / \text{cm}^2$ at the hetero-interface of the strained *n*- $\text{In}_{0.4}\text{Ga}_{0.6}\text{N}$ window layer and the *n*- $\text{In}_{0.65}\text{Ga}_{0.35}\text{N}$ emitter layer, the downward bending of bands and accumulation of electron in the region close to the interface increases the electron concentration and lowers the energy barrier both for the electron tunneling and thermionic emission, thus it can actually facilitate the collection of photo-generated electrons. Therefore, it is a key to employ the *n-on-p* InGaN cell structure rather than the *p-on-n* one to avoid or even take advantage of the effect of polarization to achieve InGaN based solar cells with high photovoltaic conversion efficiency. Note that in the above two calculations a lower dislocation density of $10^5 / \text{cm}^2$ is assumed, and so the corresponding minority carrier (electron and hole) lifetimes are used (fig. 3).

Fig. 3 shows the variation of the minority carrier lifetime with the dislocation density in above *n-on-p* InGaN solar cell. The minority carrier lifetime of electrons in $p\text{-In}_{0.65}\text{Ga}_{0.35}\text{N}$ base layer is 10^{-8} s when the dislocation density is lower than $10^5 / \text{cm}^2$ and starts to decrease rapidly to 10^{-13} s as the dislocation density increases from $10^6 / \text{cm}^2$ to $10^{11} / \text{cm}^2$. The minority carrier lifetime of holes in $n\text{-In}_{0.65}\text{Ga}_{0.35}\text{N}$ emitter layer is $7 \times 10^{-8} \text{ s}$ when the dislocation density is lower than $10^7 / \text{cm}^2$ and starts to decrease rapidly to 10^{-11} s as the dislocation density increases from $10^7 / \text{cm}^2$ to $10^{11} / \text{cm}^2$, comparable with the experimental value $\sim 470\text{ps}$ of $\text{In}_{0.08}\text{Ga}_{0.92}\text{N}$ [14].

The minority carrier lifetime of electrons is more sensitive to that of holes due to its larger diffusion coefficient. The effect of dislocation densities on the performance of $\text{In}_{0.65}\text{Ga}_{0.35}\text{N}$ single junction solar cell is calculated and presented in figure 4. It is shown that the efficiency and V_{oc} decreases gradually with the dislocation

densities increasing from $10^4 / \text{cm}^2$ to $10^{11} / \text{cm}^2$, and J_{sc} does not show obvious change until the dislocation density is high up to $10^8 / \text{cm}^2$. However, it is surprising that the fill factor initially slightly increases with the dislocation densities from $10^4 / \text{cm}^2$ to $10^6 / \text{cm}^2$, and then decrease quickly.

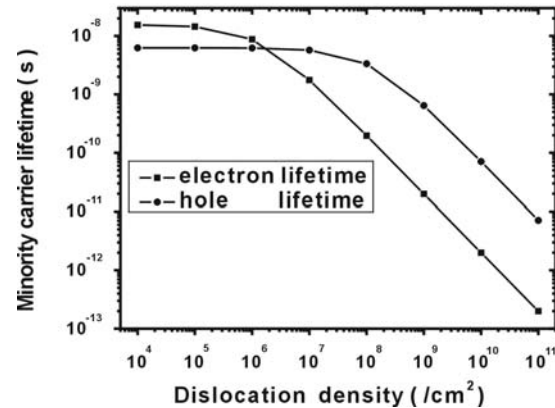


Fig. 3. The change of minority carrier lifetime versus the dislocation density in $\text{In}_{0.65}\text{Ga}_{0.35}\text{N}$ single junction solar cell. The square represents the minority carrier (electron) lifetime in the $p\text{-In}_{0.65}\text{Ga}_{0.35}\text{N}$ layer, and the dot represents the minority carrier (hole) lifetime in the $n\text{-In}_{0.65}\text{Ga}_{0.35}\text{N}$ layer.

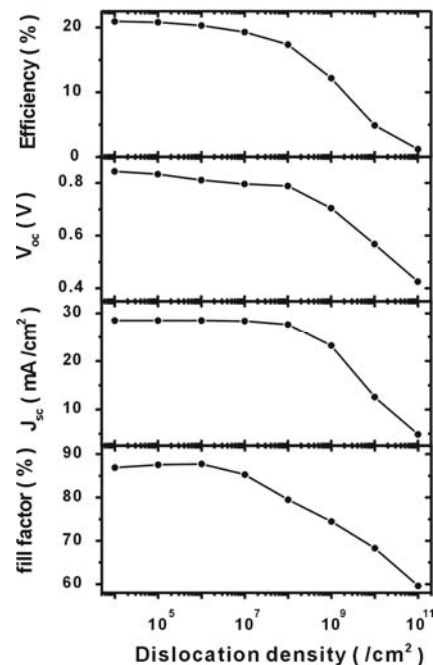


Fig. 4. The calculated performance parameters, such as efficiency, V_{oc} , J_{sc} and fill factor, of the *n-on-p* type $\text{In}_{0.65}\text{Ga}_{0.35}\text{N}$ single junction solar cell, as functions of the dislocation density.

Fig. 5 shows the relationship between the normalized efficiencies of solar cells and their corresponding dislocation densities for the $\text{In}_{0.65}\text{Ga}_{0.35}\text{N}$ and the

traditional GaAs solar cells. The data of the performance degradation of GaAs solar cell caused by the dislocations are cited from reference 15. We can see that dislocations limit the efficiency of solar cells made from both of these materials, however the efficiency of GaAs solar cell has a greater degradation rate than that of $\text{In}_{0.65}\text{Ga}_{0.35}\text{N}$ solar cell. A typical III-nitrides epilayers grown on sapphire has a dislocation density between $10^9 \sim 10^{10} / \text{cm}^2$; such high density of dislocations already leads to nearly no photovoltaic effect for GaAs solar cells, but only result in about 50% efficiency drop for the of $\text{In}_{0.65}\text{Ga}_{0.35}\text{N}$ solar cell. Therefore, it is very promising to use InGaN material system to produce high performance solar cells, just like they can be used to produce high efficiency LEDs regardless of high density of dislocations.

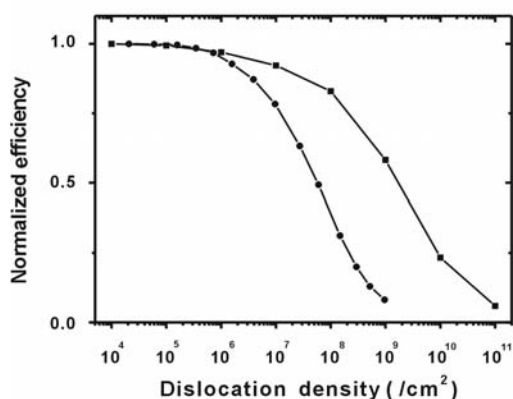


Fig. 5. Normalized efficiency for $\text{In}_{0.65}\text{Ga}_{0.35}\text{N}$ single junction solar cell (square) and GaAs single junction solar cell (dot) as a function of dislocation density. The data for GaAs single junction solar cell are cited from reference 15.

4. Conclusion

It has been shown that higher energy conversion efficiencies can be achieved for InGaN single junction solar cells with a window layer if the *n-on-p* type device structure is adopted instead of the *p-on-n* counterpart. The single biggest advantage for *n-on-p* type structure is that it can effectively avoid the adverse effects of polarization on minority carrier collection as encountered in the *n-on-p* structure. We also have revealed that the defect tolerance level of InGaN based solar cell is greater than that of GaAs solar cell, indicating that it is possible to fabricate high efficiency InGaN based solar cells in spite of high density of dislocations in this material system.

Acknowledgments

This work was supported by the Doctoral Program Foundation of Institutions of Higher Education of China (Grant No. 200804871144), the Program for New Century Excellent Talents in University (NCET-08-0214), the

Hubei Province Science Fund for Distinguished Young Scholars (Grant No.2008CDB334), the Key Programs of the Natural Science Foundation of Huazhong University of Science and Technology (Grant No. 20072008B), the National Natural Science Foundation of China (Grant No.60976042), the Open Project of State Key Laboratory of Functional Materials for Informatics, and the National Natural Science Foundation of China (Grant No. 60906023), and the National Basic Research Program of China (973 Program: 2010CB923204).

References

- [1] C. J. Neufeld, N. G. Toledo, S. C. Cruz, M. Lza, S. P. DenBaars, U. K. Mishra, *Appl. Phys. Lett.* **93**, 143502 (2008).
- [2] J. Wu, W. Walukiewicz, K. M. Yu, W. Shan, J. W. Ager III, E. E. Haller, H. Lu, W. J. Schaff, W. K. Metzger, S. Kurtz, *J. Appl. Phys.* **94**, 6477 (2003).
- [3] R. Singh, D. Doppalapudi, T. D. Moustakas, L. T. Romano, *Appl. Phys. Lett.* **70**, 1089 (1997).
- [4] X. Chen, K. D. Matthews, D. Hao, W. J. Schaff, L. F. Eastman, *Phys. Stat. Sol.* **205**, 1103 (2008).
- [5] H. Hamzaoui, A. S. Bouazzi, B. Rezig, *Sol. Energy Mater. Sol. Cells* **87**, 595 (2005).
- [6] L. Hsu, W. Walukiewicz, *J. Appl. Phys.* **104**, 024507 (2008).
- [7] B. R. Jampana, A. G. Melton, M. Jamil, N. N. Faleev, R. L. Opila, I. T. Ferguson, C. B. Honsberg, *IEEE Electron Device Lett.* **31**, 32 (2010).
- [8] O. Ambacher, J. Smart, J. R. Shealy, N. G. Weimann, K. Chu, M. Murphy, W. J. Schaff, L. F. Eastman, R. Dimitrov, L. Wittmer, M. Stutzmann, W. Rieger, J. Hilsenbeck, *J. Appl. Phys.* **85**, 3222 (1999).
- [9] S. D. Lester, F. A. Ponce, M. G. Craford, D. A. Steigerwald, *Appl. Phys. Lett.* **66**, 1249 (1995).
- [10] Z. Q. Li, Y. G. Xiao, Z. M. Simon Li, *Phys. Stat. Sol.* **4**, 1637 (2007).
- [11] T. T. Mnatsakanov, M. E. Levinshtein, L. I. Pomortseva, S. N. Yurkov, G. S. Simin, M. Asif Khan, *Solid-State Electron* **47**, 111 (2003).
- [12] J. Wu, W. Walukiewicz, K. M. Yu, J. W. Ager III, E. E. Haller, H. Lu, W. J. Schaff, *Appl. Phys. Lett.* **80**, 4741 (2002).
- [13] V. Fiorentini, F. Bernardini, O. Ambacher, *Appl. Phys. Lett.* **80**, 1204 (2002).
- [14] R. Aleksiejūnas, M. Sūdžius, V. Gudelis, T. Malinauskas, K. Jarašiūnas, Q. Fareed, R. Gaska, M. S. Shur, J. Zhang, J. Yang, E. Kuokštis, M. A. Khan, *phys. stat. sol. (c)* **0**, 2686 (2003).
- [15] M. Yamaguchi, C. Amano, *J. Appl. Phys.* **58**, 3601 (1985).

*Corresponding author: zhihao.wu@mail.hust.edu.cn